Published in final edited form as:
J Biol Chem. 2007 August 17; 282(33): 24294–24301. doi:10.1074/jbc.M703618200.

Patch Clamp and Phenotypic Analyses of a Prokaryotic Cyclic Nucleotide-gated K^+ Channel Using *Escherichia coli* as a Host*

Mario Meng-Chiang Kuo[‡], **Yoshiro Saimi**[§], **Ching Kung**[§,¶], and **Senyon Choe**[‡,1]

[‡]Structural Biology Laboratory, The Salk Institute, La Jolla, California 92037

[§]Laboratory of Molecular Biology, University of Wisconsin-Madison, Madison, Wisconsin 53706

[¶]Department of Genetics, University of Wisconsin-Madison, Madison, Wisconsin 53706

Abstract

Prokaryotic ion channels have been valuable in providing structural models for understanding ion filtration and channel-gating mechanisms. However, their functional examinations have remained rare and usually been carried out by incorporating purified channel protein into artificial lipid membranes. Here we demonstrate the utilization of *Escherichia coli* to host the functional analyses by examining a putative cyclic nucleotide-gated K^+ channel cloned from *Magnetospirillum magnetotacticum*, MmaK. When expressed in wild-type *E. coli* cells, MmaK renders the host sensitive to millimolar concentrations of externally applied K^+, indicating MmaK forms a functional K^+ conduit in the *E. coli* membrane *in vivo*. After enlarging these cells into giant spheroplasts, macro- and microscopic MmaK currents are readily detected in excised *E. coli* membrane patches by a patch clamp. We show that MmaK is indeed gated by submicromolar cAMP and ~10-fold higher concentration of cGMP and manifests as an inwardly rectified, K^+-specific current with a 10.8 pS unitary conductance at −100 mV. Additionally, MmaK is inactivated by slightly acidic pH only from the cytoplasmic side. Our *in vitro* biophysical characterizations of MmaK correlate with its *in vivo* phenotype in *E. coli*, implicating its critical role as an intracellular cAMP and pH sensor for modulating bacterial membrane potential. Exemplified by MmaK functional studies, we establish that *E. coli* and its giant spheroplast provide a convenient and versatile system to express foreign channels for biophysical analyses that can be further dovetailed with microbial genetics.

Recent sequencing of bacterial genomes reveals that ion channels evolved as early as three billion years ago. K^+ channels, for example, are widely spread in all life forms, *Bacteria*, *Archaea*, and *Eukarya* (1, 2). Because prokaryotic channel genes can often be heterologously expressed in *Escherichia coli* at high yield, the channel proteins so produced have laid an inroad to determine their crystal structures. Beginning with the prelude of MacKinnon and Doyle (3) crystal structures of these channels have raised our understanding of the molecular bases of ion channels as illustrated in several atomic structures of prokaryotic K^+ channels (4–9).

Functional interpretation of prokaryotic channel structures by electrophysiological methods, however, has not been straightforward. The main technical barrier is that the prokaryotic channel activities are often difficult to analyze under the existing methodology. A common

*This work was supported by National Institutes of Health Grants GM74821 (to S. C.), GM054867 (to Y. S.), and GM047856 (to C. K.) and the Vilas Trust of the University of Wisconsin-Madison.

[1]To whom correspondence should be addressed: 10010 N. Torry Pines Rd., La Jolla, CA 92037. Fax: 858-452-3683; choe@salk.edu.

strategy has been reconstitution of the purified channel protein into artificial lipids for bilayer lipid membrane measurement (5, 10, 11), a process that relies on the chance survival of the channel during detergent extraction and lipid reconstitution. In some cases, the reconstituted channel activities can only be demonstrated with the low resolution $^{86}Rb^+$ uptake assay (9, 12–14).

An often overlooked opportunity to capture these channels in action is the very membrane of the *E. coli* cells in which they are commonly overproduced. Although the rod of this bacterium (0.75-μm diameter, 2 μm in length) is about the dimension of a patch clamp pipette tip, there are genetic and pharmacological ways of generating giant *E. coli* some ten times its original size. In 1987, Martinac *et al.* (15) first described the enlargement of *E. coli* into giant spheroplast for direct patch clamp examination of the native mechanosensitive channels (16). Besides mechanosensitive channels, however, this pioneering method has seldom been extended to study the activities of other foreign channels. We have optimized the methods of functional preparation of giant *E. coli* spheroplast as well as patch clamp of the enlarged membrane to study MthK, the RCK (regulating the conductance of K^+)-containing K^+ channel from *Methanobacterium thermoautotrophicum* (5). The success in detecting the ensemble current of MthK in *E. coli* membrane led us to discover its hitherto unknown properties, including deactivation, desensitization, acidic inactivation, and Cd^{2+} activation (17). In this report, we illustrate the optimized method of giant spheroplast preparation and gigOhm seal formation in detail by functional expression and biophysical characterization of a bacterial cyclic nucleotide-gated K^+ channel, MmaK[2] from *M. magnetotacticum*. Related extension of microbial genetics to ion channel research is also discussed.

EXPERIMENTAL PROCEDURES

Molecular Biology and Phenotype Analysis

The *mmaK* gene (NCBI 46202428) from *M. magnetotacticum* (genomic DNA from Dr. B. Martinac, University of Queensland, Australia) was inserted into the pB13d vector between the NcoI and XhoI sites. An I2V mutation was made to create an NcoI site. The pB13d vector was created by replacing the *LacUV5* promoter and the *lac*I gene of the pB11d vector with an *E. coli* genomic fragment containing *araBAD* promoter and the *ara*C gene, corresponding to the DNA position of 70082–71319 of the *E. coli* K-12 genome. The plasmids were transformed into the TOP10 *E. coli* strain (F-, *mcr*A, Δ(*mrr-hsd*RMS-*mcr*BC), ϕ80*lac*ZΔM15, Δ*lac*X74, *deo*R, *nup*G, *rec*A1, *ara*D139, Δ(*ara-leu*)7697, *gal*U, *gal*K *rps*L(Str^R), *end*A1, λ^-, from Invitrogen) by electroporation and stored at −80 °C in the presence of 16% glycerol as a stock. Note that TOP10 has no deletions of the channels native to *E. coli*. We found it unnecessary to use *mscL*$^-$ *mscS*$^-$ bacteria for the expression of foreign channel. The presence of these mechanosensitive channels (15, 16) is in fact useful to help judge the quality of the patch (see below). For plasmid retention, 100 μg/ml ampicillin was added in all subsequent culture media. The phenotype assay was carried out following the protocol as previously described (18). Tryptone medium contain 10 g/liter of tryptone (211705; Bacto Tryptone), which has ~0.5 mM contaminating K^+ (measured with a flame photometer).

[2]The abbreviations used are: Mmak, cyclic nucleotide-gated potassium channel from *M. magnetotacticum*; MloK1, *M. loti* cyclic nucleotide-gated potassium channel; CNG, cyclic nucleotide-gated ion channel; HCN, hyperpolarization-activated cyclic nucleotide-gated ion channel; CNBD, cyclic nucleotide binding domain; MES, 4-morpholineethanesulfonic acid; TM, transmembrane.

Generation of Giant E. coli Spheroplast

To make giant spheroplasts, cells were streaked out from the −80 °C stock on a Luria Bertani-agar plate (10 g/liter tryptone, 5 g/liter yeast extract, 10 g/liter NaCl, and 1.5% agar) and grown overnight to reach colony sizes ~1–2 mm in diameter. A single colony was then inoculated in 5 ml of modified Luria Bertani medium (10 g/liter tryptone, 5 g/liter yeast extract, and 5 g/liter NaCl) in a 14-ml test tube and incubated aerobically by rotating at 250 rpm, 37 °C until A_{600} reached 0.3–0.5. At the desired A_{600}, 0.5 ml of the exponentially growing culture was diluted 10-fold into 4.5 ml of prewarmed modified Luria Bertani medium supplemented with 60 μg/ml cephalexin (diluted from 10 mg/ml of sterile stock solution) (C4895; Sigma) to block the cell fission. After 2 h of incubation by rotation at 250 rpm, 37 °C, 0.001% L-arabinose (diluted from 1% sterile stock solution) was added to the culture to induce the expression of *mmaK* for 1.5–2 h. Unseptated filaments were harvested by spinning down 1–2 ml of the culture at 3,000 ×*g* in a 1.5-ml Eppendorf tube for 1 min. The snake pellet was then resuspended with 500 μl of 0.8 M sucrose by inverting the tube a few times. 30 μl of 1 M Tris-HCl, pH 8.0, 24 μl of 0.5 mg/ml lysozyme (~20 μg/ml final concentration (~600 units) (L6876; Sigma)) 6 μl of 5 mg/ml DNase (~50 μg/ml final concentration (D5025; Sigma)), and 6 μl of 125 mM EDTA-NaOH, pH 8.0 (~1.3 mM final concentration) were added in sequence and mixed immediately in between by inverting the tube a few times. After 5–10 min of incubation at room temperature, 100 μl of Stop Solution (10 mM Tris-HCl, pH 8.0, 0.7 M sucrose, 20 mM $MgCl_2$) was added to terminate digestion. The spheroplasts were directly used for patch clamping or frozen in aliquots at −80 °C and thawed in ice before later usage. We found that the amount of the lysozyme and EDTA described previously (15, 19) tends to produce transparent or grayish spheroplasts on which it is difficult to form gigOhm seals. Lowering the concentrations as described herein increases the consistency of the qualities of the giant spheroplasts in our applications.

Recording Set-up and Formation of gigOhm Seal

A calibrated glass pipette (100-μl; catalog number 2-000-100; Drummond Scientific Company, Broomall, PA) was pulled in two steps to a tip size ~4.5–5.0 bubble number (usually ~7–3 MΩ in the K150 solution) with a P-97 Micropipette Puller (Sutter Instrument Company, Novato, CA) and filled with a pipette solution (K150, pH 7.5, containing 10 mM Hepes-Tris, pH 7.5, 150 mM KCl, 20 mM $CaCl_2$, and 500 mM sucrose), except for Fig. 6*B*, which was filled with a K150, pH 5.5, solution. The same solution was added to a patch clamp chamber (RC-22; Warner Instruments, Hamden, CT) together with 0.5–1 μl of the giant spheroplasts. Note that the addition of 20 mM Ca^{2+} (or Mg^{2+}) in the pipette and bath solutions is necessary for gigOhm seal formation. We found that lowering the concentration of these divalent ions below millimolar range significantly affects the ability to obtain gigOhm seal. Under an inverted microscope (Nikon Eclipse TE300) equipped with ×10 ocular lenses and a ×40 phase contrast objective, the giant spheroplasts appear in different sizes and darkness. Note that not all the giant spheroplasts are adequate to form a gigOhm seal. We found that the giant spheroplasts with black or dark gray color are easier to form gigOhm seal than the transparent or grayish ones. With sufficient magnification under phase contrast (usually requires higher than ×200), coils of ruptured outer membrane can be visualized as rough materials around the surface, which should be excluded from the patch. The seal formation was monitored under the Seal Test window of a Clampex 8.1 software (Axon Instruments, Sunnyvale, CA). After initial attachment to the membrane and suction of the pipette by mouth, the seal resistance usually increased to ~20–50 megOhm rapidly. With continual application of negative pressure to the pipette by mouth, the seal resistance increased to ~1–2 gigOhm in a few seconds to minutes. We found that continuously holding the membrane at positive potentials (20–50 mV under the Gap-free mode of the Clampex 8.1 software) can often stabilize the seal and further increase the seal resistance to higher than 3 gigOhm in a few minutes. A membrane patch was then excised from the giant

spheroplast by gently tapping the micromanipulator (Leica) that held the headstage of an EPC7 Patch Clamp Amplifier (HEKA Instruments, Southboro, MA). After excision of a membrane patch, gentle suctions by mouth were applied to the patch to confirm the presence of the standard mechanosensitive channel activities (usually MscS, mechanosensitive channel of small conductance) (15, 16) that serve as an internal control of correct membrane configuration. No pressure was applied to the membrane path afterward. The pipette tip was then positioned in front of the opening of a single-walled, 3-barrel glass tube (0.7 mm ID) of the SF-77B perfusion system (Warner Instruments, Hamden, CT). The perfusates were gravity-fed, and the flow speed at the opening of the tubing was estimated to be ~0.5 cm/s. Stepping of the perfusion channels was controlled by programmed protocols (Episodic stimulation mode) through an analog OUT channel in the Clampex 8.1 software and a Digidata1322A digitizer (Axon Instruments). The analog stepping signal was digitized and recorded together with those of the probe voltage and the membrane current for data analysis using a Clampfit 9.2 software (Axon Instruments). Before being digitized, the analog current signal was filtered inline with an 8-pole Bessel filter (Frequency Devices Inc., Haverhill, MA). The dead time (from the beginning of the stepping to the activation of channels) varied between 30 and 110 ms from patch to patch. This variation may be due to the varied pipette tip sizes and the distance between the membrane patch and the opening of the pipette tip. All the solutions containing sucrose were sterilized by 0.2-μm filtration and stored at room temperature. Concentrated nucleotide stocks were diluted into the perfusate before usage.

RESULTS

Strategy of Examining Foreign Channel Activity in E. coli

Fig. 1 summarizes the general methods of using *E. coli* to host the functional analyses of a foreign ion channel. Using BLAST (Basic Local Alignment Search Tool), we have compiled subtypes of prokaryotic K^+ channel genes available from known bacterial and archaeal genomes (1). The desired channel gene is retrieved through PCR from the genomic DNA of the original organism and transformed into an *E. coli* strain for heterologous expression. Whether the channel gene produces a functional K^+ conduit in the *E. coli* membrane can be surveyed *in vivo* by looking for K^+-related phenotypes and *in vitro* by directly enlarging the same cells for patch clamping to detect the corresponding current.

As an example, gene homologues of animal cyclic nucleotide-gated cation channels (CNG or HCN) have been identified in a few bacterial genomes (1); however, their biophysical activities have not been successfully detected to date. One such gene homologue, *mmaK* in *M. magnetotacticum*, encodes a putative 389-residue K^+ channel subunit containing six predicted trans-membrane segments (TMs) and a cytoplasmic cyclic-nucleotide binding domain (CNBD) at the carboxyl terminus (Fig. 2). A conserved K^+ filter sequence, TVGFGD, is found between its TM5 and TM6. The entire coding sequence of *mmaK* has 90% similarity (37% identity, 53% positive) to the MloK1 channel from *Mesorhizobium loti*, whose CNBD has been crystallized and whose activity has been documented by population $^{86}Rb^+$ uptake assay (13, 14), although not by electrophysiological methods. The “C-linker” that is typically found in the animal CNG and HCN channels are absent in both of the bacterial MmaK and MloK1 channels (Fig. 2).

Expression of MmaK Renders the E. coli Host Sensitive Specifically to K^+ Ion in the Medium

The *mmaK* gene was cloned into the pB13d vector behind an *araBAD* promoter and transformed into the wild-type TOP10 *E. coli* cells. The *E. coli* host carrying the pB13d-MmaK plasmid is highly sensitive to the K^+ concentrations in the growth medium even in

the absence of the arabinose inducer (Fig. 3). On tryptone-based agarose plates, the *mmaK*-bearing cells can grow like control cells with or without added NaCl (Fig. 3*A*, *bottom rows in plates 1–3*) without losing colony-forming units (evident at the final dilution), although the colonies are thinner and therefore translucent (see "Discussion"). However, these *mmaK*-bearing cells cannot grow on plates with additional 10 or 50 mM KCl (Fig. 3*A*, *bottom rows in plates 4* and *5*, respectively), unlike the control (*top rows in plates 4* and *5*). This K^+-sensitive phenotype is also observed in liquid medium. Adding 10 mM KCl to the exponentially growing cultures immediately stops the growth of the *mmaK*-bearing cells (Fig. 3*B*, *filled circles* in *panel 3*), but not the control cells (*open circles*). This growth inhibition in liquid medium is also specific to K^+, but not to Na^+, because adding equal molar NaCl has no effect on the growth of both cell types (Fig. 3*B*, *panel 2*). This K^+-sensitive phenotype is very similar to that caused by the gain-of-function mutants of the native *Kch* channel of *E. coli* (18), indicating that the *E. coli* cells are able to express MmaK and to form a functional K^+ conduit in its membrane. Note that the K^+-sensitive phenotype observed in both cases was carried out in the absence of the corresponding inducers, reiterating that the leakage levels of the inducible promoters are enough to produce sufficient number of channels to give the observable phenotypes. This K^+ sensitivity is the first reported phenotype caused by a foreign K^+ channel gene in a wild-type *E. coli*, although others have shown rescue phenotypes of a K^+ auxotroph (20–24).

Patch Clamp Analyses of MmaK in Enlarged E. coli Membrane

Because the *in vivo* phenotyping assay indicates that MmaK can be functionally expressed in *E. coli*, we then went on to test whether a corresponding K^+-specific current can be detected on the *E. coli* membrane. The same *mmaK*-bearing cells were thus enlarged as giant spheroplasts for direct patch clamp analysis. L-Arabinose, the inducer of the *araBAD* promoter, was added to promote the expression and to maximize our chances of finding the corresponding current. The basic method of enlarging *E. coli* cells (15, 19) has been optimized for consistent giant spheroplast and gigOhm seal formation. To this end, we found the concentrations of lysozyme and EDTA to be critical (see "Experimental Procedures"). High resolution optics were adopted here to visually select the debris-free surface to increase the rate of obtaining gigOhm seals. Because MmaK contains a CNBD at its cytoplasmic carboxyl terminus, we employed the excised inside-out patch mode to allow presentation of the putative ligand, cAMP and cGMP. To resolve ligand activation time course, a rapid perfusate stepping system was also adopted to ensure rapid solution exchanges in tens of milliseconds.

MmaK Is Gated by Submicromollar cAMP and Micromollar cGMP from the Cytoplasmic Side

In a frequency of ~nine of ten excised patches examined, a cAMP-inducible macroscopic current is readily observed when a stream of perfusate containing 100 μM cAMP is brought to bathe the patch ($n > 70$, Fig. 4*A*, *left*), whereas the cells carrying the control empty vector have never shown this activity ($n > 10$, data not shown). The number of unitary conductance in an excised patch varies ~30 –300, although patches containing more than 600 units have also been observed occasionally. The cAMP activation and deactivation kinetics can each be fitted with a single exponential with a τ of 26.9 ± 9.3 ms and 1.77 ± 0.33 s, respectively (n = 13) (Fig. 4*A*, *right*). These fast activation and slow deactivation kinetics are similar to those of eukaryotic CNG channels (25), implicating a compatible gating mechanism involving the cyclic nucleotide binding domain, even though the bacterial MmaK channel does not contain the C-linker between its TM6 and the CNBD (Fig. 2). The cAMP dose response was examined between 0.1 and 100 μM and revealed a half-effective concentration (EC_{50}) of 0.72 μM and a Hill coefficient (h) of ~1.2 (n = 5, Fig. 4*B*). Cyclic GMP apparently also

activates MmaK, but with ~10-fold less efficacy than cAMP does (EC_{50} ~ 7.4 μM and h ~ 1.5, n = 2, Fig. 4*B*, *right*).

Besides the ensemble currents, the unitary current of MmaK was also observed after the deactivation of most of the channels in the ensemble. This microscopic unitary current reveals a unitary conductance of 10.8 pS at −100 mV of membrane potential (Fig. 4*C*). This is the first unitary conductance of a prokaryotic cAMP-activated K^+ channel reported, and it is apparently larger than those of the eukaryotic HCN cation channels (26).

MmaK Conducts an Inwardly Rectified, K^+-selective Current

The ion-conducting properties of the cAMP-induced MmaK current were examined by ramping the holding membrane potential from −150 to +150 mV. With 150 mM KCl at both sides of the membrane, we found that the current rectifies inwardly beginning near 0 mV, indicating the channel is voltage-sensitive in addition to being cAMP-activated (Fig. 5*A*, the *K150 trace*). MmaK contains a K^+ filter sequence, TVGFGD, between TM5 and TM6 (Fig. 2). To test whether MmaK is selective for K^+ ion, we replaced the KCl with NaCl perfusate and found that the latter reversibly abolishes the outward current (Fig. 5*A*, the *Na150 trace*, and 5*B*), indicating the channel indeed does not pass Na^+. Thus, MmaK is likely to conduct K^+ in the deep polarized membrane potential of the bacterium, explaining the *in vivo* phenotype above (Fig. 3, see also “Discussion”).

MmaK Is Inactivated by Slightly Acidic pH but Only from the Cytoplasmic Side

Several prokaryotic K^+ channels are known to be regulated by pH (12, 17, 27, 28). To see whether the activity of MmaK is also modulated by pH, we perfused the cytoplasmic-side-out membrane patch with perfusates containing various pH values from 8.5 to 5.5. We found that MmaK is reversibly inactivated by slightly acidic pH values with a half inactivation pH of 7.0 and a Hill coefficient of 0.79 (n = 5, Fig. 6*A*). This acid inactivation only happens when the low pH is applied to the cytoplasmic side, because reducing the pH of the pipette solution to 5.5 does not inactivate MmaK (Fig. 6*B*). These results indicate that the pH-sensing module of the MmaK channel is located intracellularly.

By patch clamping the MmaK channel in the *E. coli* membrane, we found MmaK can reside in at least three functional states: closed, open, and acid-inactivated (Fig. 6*C*). The functionality of this bacterial cyclic nucleotide-gated K^+ channel is apparently similar to other eukaryotic or prokaryotic K^+ channels, having a sizable unitary conductance and being an intricate sensor of various metabolic and environmental signals: nucleotides, pH, and voltage.

DISCUSSION

In this report, we demonstrated that the model *E. coli* bacterium can be comparable with *Xenopus* oocyte as an arena for heterologous ion channel expression and characterization, in addition to its traditional role as the factory to produce foreign recombinant proteins. The ability to directly examine the electrophysiology of foreign prokaryotic ion channels in enlarged *E. coli* membrane (17, 29, 30) provides several technical advantages over the existing eukaryotic expression systems or reconstitutions. First, for prokaryotic channels, there is a better chance of their being functionally expressed in *E. coli*, a fellow prokaryote, than in eukaryotic cells. Second, giant spheroplasts can be prepared with relative ease, obviating the need of mRNA synthesis for injection or protein purification for reconstitution. Third, the reconstitution procedure has little control over how the channel protein is inserted into the artificial membranes, leading to possible questions on the orientation of the assembled channels. Because a giant spheroplast is essentially a large cell, there is no

ambiguity in sidedness for on-cell or excised patches used. Forth, excised patches, together with rapid perfusion, allow resolution of the time course of channel activation, deactivation, and inactivation by ligands (*e.g.* Fig. 4), which is difficult to achieve with the technique of conventional planar lipid bilayer. Fifth, once generated, giant spheroplasts can be stored at −80 °C and be thawed for patch clamping without having to reinitiate preparation. Months of storage apparently have no detrimental effects on channel activities. Sixth, and most importantly, the need for only one construct not only saves time and effort but also ensures that the *in vivo* observations (phenotype) correspond to the *in vitro* ones (biophysics). Because the very same bacterial strain can now be examined on plate by genetics and under the electrode by biophysics, efficient cycling between the two powerful enterprises is anticipated.

A plate or tube phenotype is invaluable in microbial genetics to study the *in vivo* functions of a gene product. As shown in Fig. 2, MmaK renders *E. coli* sensitive to externally added K^+, but not Na^+. This K^+-sensitive phenotype recapitulates the gain-of-function phenotype discovered after mutagenizing *Kch*, the gene that encodes the K^+ channel native to *E. coli* (18). Externally enriched K^+ apparently causes membrane depolarization through the gain-of-function *Kch* channels, resulting in the K^+-specific growth phenotype (31). That *mmaK*-bearing cells phenocopy gain-of-function *kch*-bearing cells suggests a similar pathogenic mechanism (Fig. 7). The cellular cAMP of *E. coli* is known to vary between 0.5 and 10 μM (32). Here, we found the EC_{50} of cAMP in MmaK activation to be ~0.72 μM under patch clamp. Thus, this biophysical property *in vitro* is entirely compatible with the K^+-sensitive phenotype *in vivo*, indicating that MmaK is constitutively activated by the cAMP in the host cells. This constitutive activity is reflected even in live cells grown in ordinary tryptone medium containing only ~0.5 mM of contaminating K^+. Note that such cells grow to lower final density in liquid medium (Fig. 3*B*, *panels 1* and *2*) and make thin and therefore translucent colonies on plate (Fig. 3*A*, *plates 1*, *2*, and *3*), indicative of stress. We believe that MmaK channels in effect clamp the membrane potential (V_m) at or near the equilibrium potential of K^+ (E_K). This is tolerated when E_K is reasonably deep as in ordinary medium, but the V_m would become too shallow (hypopolarized) for growth when E_K is reduced by externally added K^+ (Fig. 7). Therefore, it is likely that MmaK functions as a cytoplasmic cAMP sensor in transducing the chemical signal into electric ones (V_m or protonmotive force) in the original organism.

It is now possible to isolate gain- or loss-of-function MmaK mutations and directly correlate the biophysical alternations they cause with the amino acid substitutions. Further second-site intragenic suppressor mutations may give insights into amino acid interactions during gating. These assumption-free forward genetic methods, together with site-directed reverse genetics as predicted by sequence or crystal structure and spheroplast patch clamp, promise even deeper understanding of the structure-function relationship of ion channels.

Acknowledgments

We thank Dr. B. Martinac for the generous gift of M. magnetotacticum DNA.

References

1. Kuo MMC, Haynes WJ, Loukin SH, Kung C, Saimi Y. FEMS Microbiol Rev. 2005; 29:961–985. [PubMed: 16026885]
2. Loukin SH, Kuo MMC, Zhou XL, Haynes WJ, Kung C, Saimi Y. J Gen Physiol. 2005; 125:521–527. [PubMed: 15897296]
3. MacKinnon R, Doyle DA. Nat Struct Biol. 1997; 4:877–879. [PubMed: 9360597]

4. Doyle DA, Cabral JM, Pfuetzner RA, Kuo AL, Gulbis JM, Cohen SL, Chait BT, MacKinnon R. Science. 1998; 280:69–77. [PubMed: 9525859]
5. Jiang YX, Lee A, Chen JY, Cadene M, Chait BT, MacKinnon R. Nature. 2002; 417:515–522. [PubMed: 12037559]
6. Jiang YX, Lee A, Chen JY, Ruta V, Cadene M, Chait BT, MacKinnon R. Nature. 2003; 423:33–41. [PubMed: 12721618]
7. Kuo A, Gulbis JM, Antcliff JF, Rahman T, Lowe ED, Zimmer J, Cuthbertson J, Ashcroft FM, Ezaki T, Doyle DA. Science. 2003; 300:1922–1926. [PubMed: 12738871]
8. Kuo AL, Domene C, Johnson LN, Doyle DA, Venien-Bryan C. Structure. 2005; 13:1463–1472. [PubMed: 16216578]
9. Shi N, Ye S, Alam A, Chen L, Jiang Y. Nature. 2006; 440:570–574. [PubMed: 16467789]
10. Ruta V, Jiang YX, Lee A, Chen JY, MacKinnon R. Nature. 2003; 422:180–185. [PubMed: 12629550]
11. Heginbotham L, LeMasurier M, Kolmakova-Partensky L, Miller C. J Gen Physiol. 1999; 114:551–560. [PubMed: 10498673]
12. Enkvetchakul D, Bhattacharyya J, Jeliazkova I, Groesbeck DK, Cukras CA, Nichols CG. J Biol Chem. 2004; 279:47076–47080. [PubMed: 15448150]
13. Clayton GM, Silverman WR, Heginbotham L, Morais-Cabral JH. Cell. 2004; 119:615–627. [PubMed: 15550244]
14. Nimigean CM, Shane T, Miller C. J Gen Physiol. 2004; 124:203–210. [PubMed: 15337819]
15. Martinac B, Buechner M, Delcour AH, Adler J, Kung C. Proc Natl Acad Sci U S A. 1987; 84:2297–2301. [PubMed: 2436228]
16. Kung C. Nature. 2005; 436:647–654. [PubMed: 16079835]
17. Kuo MMC, Baker KA, Wong L, Choe S. Proc Natl Acad Sci U S A. 2007; 104:2151–2156. [PubMed: 17287352]
18. Kuo MMC, Saimi Y, Kung C. EMBO J. 2003; 22:4049–4058. [PubMed: 12912904]
19. Blount P, Sukharev SI, Moe PC, Martinac B, Kung C. Methods Enzymol. 1999; 294:458–482. [PubMed: 9916243]
20. Sun S, Gan JH, Paynter JJ, Tucker SJ. Physiol Genomics. 2006; 26:1–7. [PubMed: 16595742]
21. Parfenova LV, Crane BM, Rothberg BS. J Biol Chem. 2006; 281:21131–21138. [PubMed: 16728395]
22. Ptak CP, Cuello LG, Perozo E. Biochemistry. 2005; 44:62–71. [PubMed: 15628846]
23. Sesti F, Rajan S, Gonzalez-Colaso R, Nikolaeva N, Goldstein SA. Nat Neurosci. 2003; 6:353–361. [PubMed: 12640457]
24. Hellmer J, Zeilinger C. FEBS Lett. 2003; 547:165–169. [PubMed: 12860407]
25. Zufall F, Hatt H, Firestein S. J Biol Chem. 1993; 90:9335–9339.
26. DiFrancesco D, Mangoni M. J Physiol. 1994; 474:473–482. [PubMed: 7516974]
27. Gao L, Mi X, Paajanen V, Wang K, Fan Z. Proc Natl Acad Sci U S A. 2005; 102:17630–17635. [PubMed: 16301524]
28. Li Y, Berke I, Chen L, Jiang Y. J Gen Physiol. 2007; 129:109–120. [PubMed: 17261840]
29. Santos JS, Lundby A, Zazueta C, Montal M. J Gen Physiol. 2006; 128:283–292. [PubMed: 16908725]
30. Nakayama Y, Fujiu K, Sokabe M, Yoshimura K. Proc Natl Acad Sci U S A. 2007; 104:5883–5888. [PubMed: 17389370]
31. Kuo, MM-C. PhD thesis. University of Wisconsin; Madison: 2005. Prokaryotic K^+ Channels: A Survey and a Case Study on the Biological Functions of the Escherichia coli Kch.
32. Botsford JL. Microbiol Rev. 1981; 45:620–642. [PubMed: 6276705]
33. Zagotta WN, Olivier NB, Black KD, Young EC, Olson R, Gouaux E. Nature. 2003; 425:200–205. [PubMed: 12968185]
34. Harold, FM.; Maloney, PC. Escherichia coli and Salmonella. Neidhardt, FC., editor. Vol. 1. ASM Press; Washington, D. C: 1996. p. 283-306.

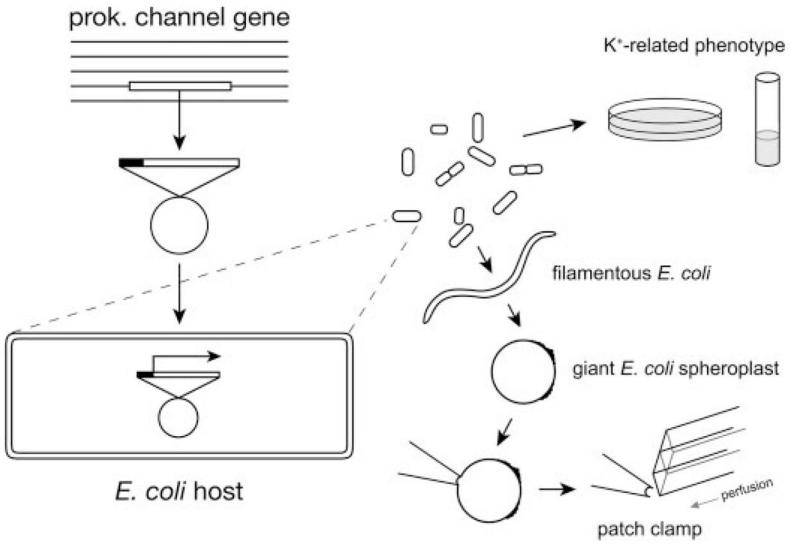

FIGURE 1. Experimental scheme of functional examinations of a foreign prokaryotic channel in *E. coli*, including phenotyping *in vivo* as well as the procedure of generating giant spheroplasts from the same cells for patch clamping *in vitro*.

The gene of interest is cloned into a bacterial vector behind an inducible promoter, and the plasmid is transformed into an *E. coli* host. Cells carrying the plasmid are subjected to growth analyses for K^+-related phenotypes. The same cells can be enlarged by first blocking the cell division with cephalexin to generate unseptated filamentous cells, which are then converted to giant spheroplasts by lysozyme and EDTA. A small patch can be excised directly from the enlarged membrane to allow electrophysiological examinations and effective ligand presentation from the cytoplasmic side. Glass tubes mounted on a stepping motor are positioned such that the patch is bathed in a perfusate, which can be switched to the alternate perfusate within tens of milliseconds.

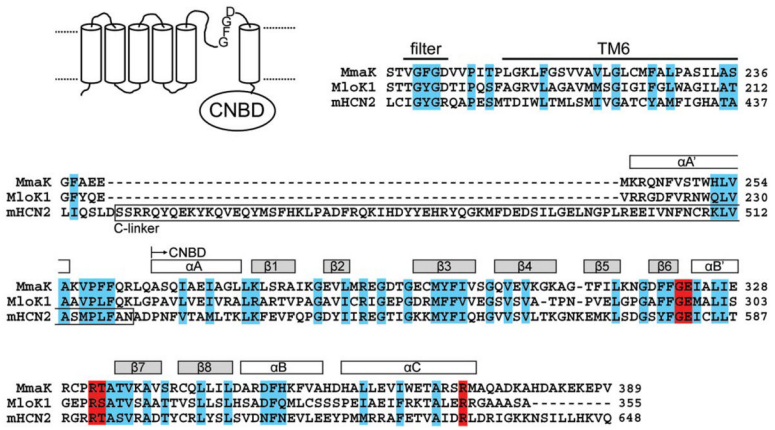

FIGURE 2. Predicted membrane topology of MmaK (NCBI 46202428) and its partial sequence alignment with the prokaryotic MloK1 channel (NCBI 13472825) and the mouse HCN2 channel (NCBI 29840777)

The alignment begins with the canonical K^+ filter sequence and ends with the cyclic nucleotide binding domain (*CNBD*). Residues with strong conservation are marked in *cyan*. The secondary structures (*rectangles above the sequences*) are based on the x-ray structure of MloK1's CNBD (PDB accession code 1VP6) (13). The cyclic phosphate coordinating residues revealed from the x-ray structures are marked in *red* (13, 33). The "C-linker" between the TM6 and CNBD typically found in the animal CNG and HCN channels is *boxed*.

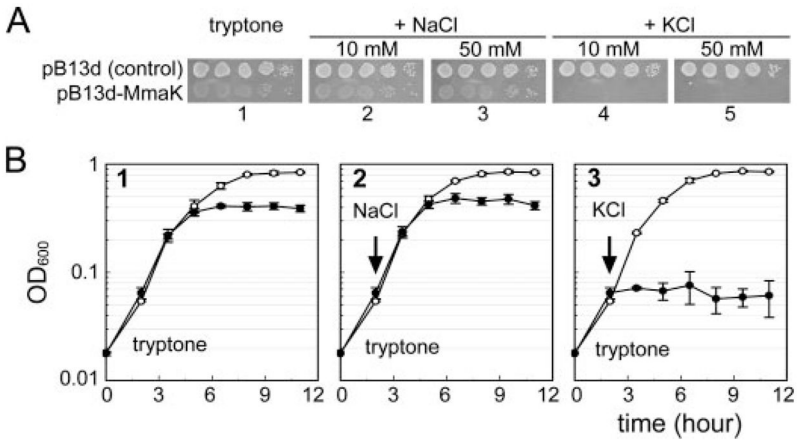

FIGURE 3. Expression of the *mmaK* renders the wild-type *E. coli* cells sensitive to externally added K^+ ion

A, phenotyping of the cells carrying the empty control plasmid (*top row*) or the pB13d-MmaK plasmids (*bottom row*) on tryptone-based agarose plates. On the plate containing only tryptone (*plate 1*) or tryptone with an additional 10 or 50 mM NaCl (*plates 2* and *3*), the colonies of *mmaK*-bearing cells are more translucent (see "Discussion"), but the colony-forming units of the *mmaK*-bearing cells are similar in *plates 1*, *2*, and *3*, indicating that these media do not restrict growth. However, on the plate containing an additional 10 or 50 mM KCl (*plates 4* and *5*), the colony-forming units of the *mmaK*-bearing cells were reduced by $>10^5$-fold. Each spot was inoculated from 5 μl of a series of 10-fold dilution of stationary cells (10^2-, 10^3-, 10^4-, 10^5-, and 10^6-fold from *left to right*). *B*, phenotype in the liquid medium and effects of adding Na^+ or K^+ to exponentially growing cultures. In the tryptone medium (*panel 1*), the growth rate of the *mmaK*-bearing cells (*filled circles*) is similar to that of the control cells (*open circles*); however, the cell density of the stationary *mmaK*-bearing cells is lower than that of the control cells. Addition of 10 mM KCl (*arrow* in *panel 3*), but not 10 mM NaCl (*panel 2*), immediately stops the growth of the *mmaK*-bearing cells, but not the control cells without *mmaK*. For the growth curve measurements, stationary cells in modified Luria Bertani medium were washed once with fresh tryptone medium and inoculated into fresh tryptone medium to A_{600} ~ 0.02 as the time "*0*", and the cultures were incubated aerobically by rotating at 275 rpm in 37 °C. Growth was monitored by measuring the optical densities at 600 nm. Data were averaged from duplicate experiments of independent transformants (standard deviations are shown).

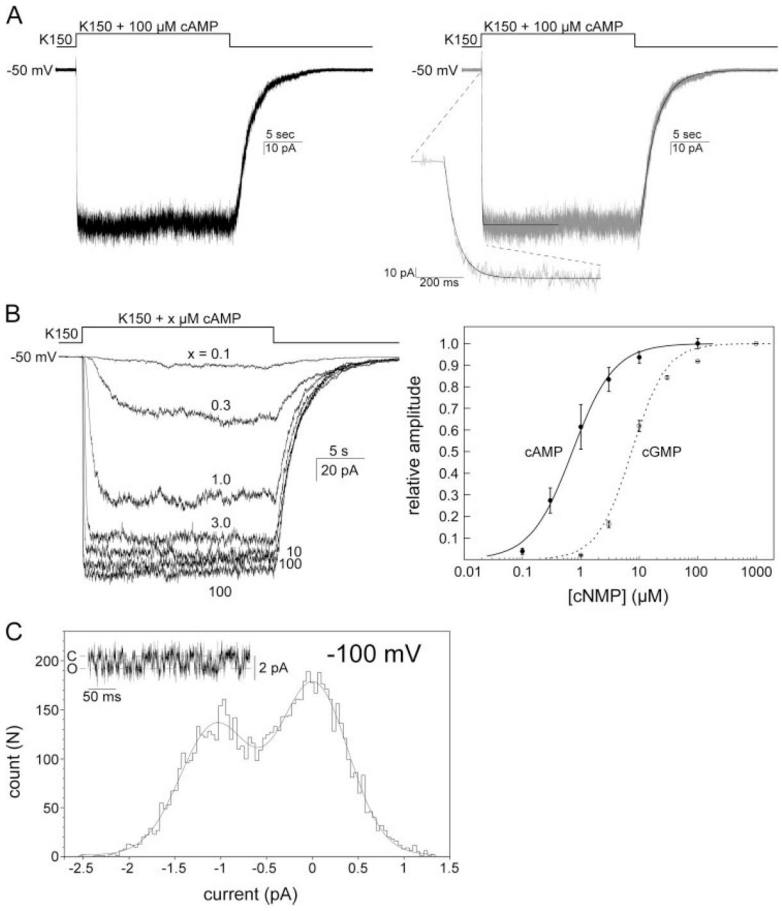

FIGURE 4. MmaK currents and cAMP and cGMP dose responses recorded from excised inside-out membrane patches of giant *E. coli* spheroplast

A, left, representative macroscopic current activated by 100 μM cAMP at −50 mV of hold potential. After excision, the patch was perfused with the K150, pH 7.5, solution and then, with a rapid perfusion system, stepped into the same K150, pH 7.5, solution containing an additional 100 μM cAMP, and finally stepped back to the first solution. Sampled at 2.5 kHz and filtered at 1 kHz. *Right*, macroscopic cAMP activation and deactivation traces, each fitted with a single exponential (*smooth lines*). Deactivation upon the withdrawal of cAMP is a relatively slow process and completes in seconds. *B,* macroscopic cAMP and cGMP dose responses. *Left*, superimposed traces of MmaK current from a same patch activated by different concentrations of cAMP. Activations were carried out in an order of 100, 0.1, 0.3, 1, 3, 10, and 100 μM. No significant run-down was observed between the first and the last 100-μM activation. Sampled at 2.5 kHz and filtered at 1 kHz (further filtered at 20 Hz for presentation here). *Right*, to obtain the cAMP dose-response curve, the peak amplitude at each concentration was determined by averaging the currents from 5 to 10 s after stepping the perfusate to the cAMP-containing solution. Relative amplitude was the ratio of the peak amplitude at each cAMP concentration and that of the averaged 100-μM activations (the first and the last). The averaged data set of five patches (*filled circles*, standard deviations are shown) was fitted with a Hill equation, $f(C) = (I_{max} \times [C]^h)/(EC_{50}{}^h + [C]^h)$, where C is the cAMP concentration, h is the Hill coefficient, and I_{max} is the maximum response (fixed at 100). The cGMP dose-response curve is shown in *empty circles* and the *dashed line. C*, amplitude histogram of the unitary current revealed after bulk deactivation at −100 mV

(*inset* shows a sample trace). The Gaussian fit (*smooth curve*) shows a unitary conductance of 10.8 pS. Sampled at 25 kHz and filtered at 2.5 kHz.

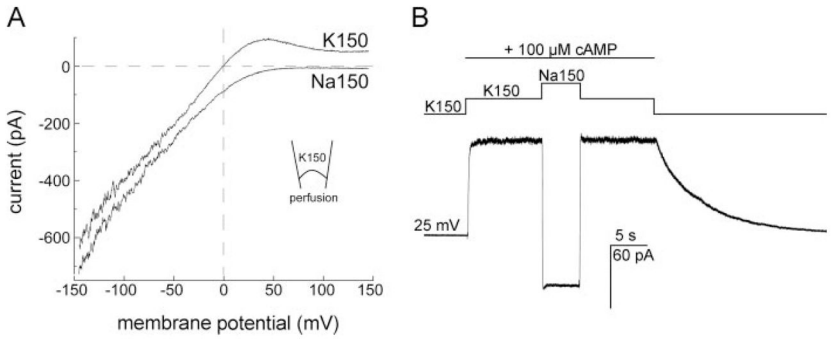

FIGURE 5. The cAMP-activated MmaK current rectifies inwardly and is K^+-specific

A, ensemble currents during a 200-ms voltage ramp from −150 to +150 mV show that the MmaK current rectifies inwardly. The ~370 channels in the excised patch were activated by 100 μM cAMP at 0 mV for 3 s before the voltage ramp was applied. Leak currents of the entire ramp in the absence of cAMP activation were subtracted. In symmetric 150 mM KCl (*K150*, *upper trace*, perfusate contains cAMP), the outward current is reduced to near zero at positive voltages above ~100 mV, indicative of inward rectification. Between 0 and +75 mV, however, outward currents are observed, indicative of open channels. (Here outward current flows from the bath, the cytoplasmic side, into the pipette.) As the voltage increases, rectification reduces the ensemble conductance while the outward electromotive force increases. This competition results in the prominent hump. Replacing the perfusate with cAMP-containing 150 mM NaCl (*Na150*, *lower trace*) eliminates this hump, indicating that the MmaK channel still rectifies but there is no outward driving force for cation when K^+ is absent. The downward displacement of the current trace in Na150 at negative voltages is also consistent with the increase in the chemical driving force of K^+ through a K^+-selective filter. Sampled at 10 kHz and filtered at 4 kHz. *B*, switching the cAMP-containing perfusate from K150 to Na150 reverses the macroscopic current at +25 mV, further illustrating that MmaK does not allow Na^+ permeation. Sampled at 1 kHz and filtered at 0.5 kHz.

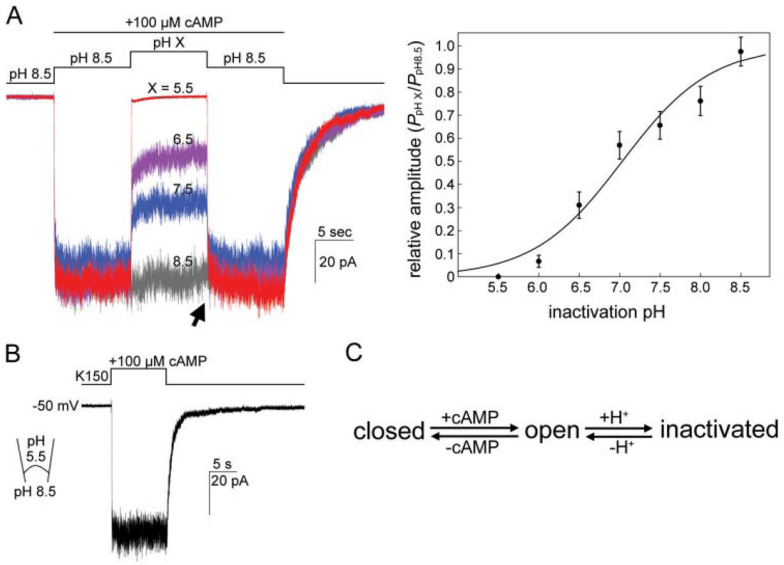

FIGURE 6. MmaK is inactivated by slightly acidic pH applied to the cytoplasmic side

A, left, superimposed traces of MmaK current in response to different pH values of the perfusate. After excision, the patch was perfused with a K150, pH 8.5, solution and stepped to the same solution containing an additional 100 μM cAMP to activate the channels. After 10 s of activation, the perfusate was then stepped to a cAMP-containing solution with various pH values. Full inactivation is observed at pH 5.5. The acid-inactivated macroscopic currents are readily restored almost fully when the pH is returned to 8.5 (*arrow*). Data were recorded for a same patch. Perfusion solutions with different pH have the same components as the K150, pH 7.5, except the buffer was replaced with citrate for pH 5.5, MES-Tris for pH 6.0 and 6.5, and Hepes-Tris for pH 7.0 to 8.5. Sampled at 1 kHz and filtered at 0.5 kHz. *Right*, to obtain the H^+ dose-response curve, the averaged data set of five patches (*filled circles*, standard deviations are shown) was fitted with a Hill equation: $I(C) = I_{min} + \{(I_{max} - I_{min})/[1 + ([C]/IC_{50})^h]\}$, where C is the H^+ concentration, h is the Hill coefficient, and I_{max} and I_{min} are the maximum and minimum responses, respectively (fixed at 100 and 0, respectively). The Hill fitting curve (*smooth line*) reveals an IC_{50} of pH 7.0 and a Hill coefficient of 0.79. *B,* MmaK remains active when the pipette is filled with a pH 5.5 solution. *C*, a summary diagram shows that MmaK transits among at least three functional states.

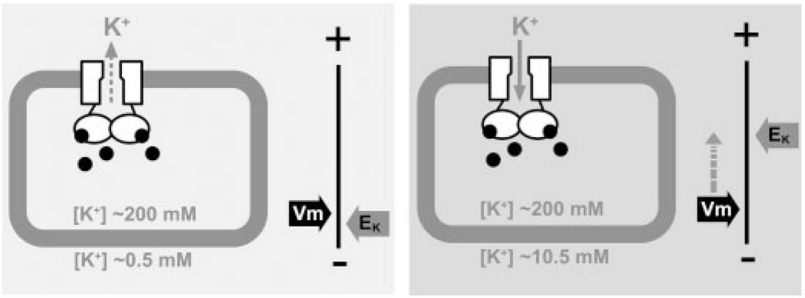

FIGURE 7. A hypothetic model to illustrate the cause of the K^+-sensitive phenotype by the cAMP-gated MmaK in the host *E. coli* cell

MmaK in the live *E. coli* is constitutively activated by the intracellular cAMP (*black dots*). Whether there is a K^+ flux through MmaK depends on the membrane potential (V_m) and the equilibrium potential of K^+ (E_K). The V_m of an aerobically growing *E. coli* cell is ~ −130 to −150 mV, which is set by active proton extrusion through the respiratory components on the cell membrane (34) *Left*, when the external [K^+] is low (~0.5 mM K^+ in the tryptone medium), the E_K is deep (~−155 mV, assuming $[K^+]_{in}$ = 200 mM). The driving force for K^+ ($\Delta\mu_K$) would be slightly positive to cause K^+ efflux through MmaK and may result in a small hyperpolarization of the V_m. *Right*, adding 10 mM K^+ to the medium increases E_K (to ~−75 mV) and decreases the $\Delta\mu_K$ (to ~−55 to −75 mV). The sizable negative $\Delta\mu_K{}^+$ would drive K^+ flux into the cell through the active MmaK and result in significant depolarization of the V_m toward E_K. Because V_m is the major component of the protonmotive force (Δp), the reduced Δp may not be able to provide enough driving force for other cellular processes, and thus the cell growth stops. The lower final density in liquid and thinner colonies on semi-solid plates suggests that the MmaK-bearing cells are under stress even in tryptone medium (Fig. 3), consistent with there being a small, albeit tolerable, $\Delta\mu_K$ even in growing cultures from the constitutively active MmaK channels.